

How East Asian westerly jet's meridional position affects the summer rainfall in Yangtze-Huaihe River Valley?

Shixin Wang¹ · Hongchao Zuo¹  · Shuman Zhao¹ · Jiankai Zhang¹ · Sha Lu¹

Received: 23 June 2016 / Accepted: 16 February 2017 / Published online: 22 March 2017
© The Author(s) 2017. This article is an open access publication

Abstract Existing studies show that the change in the meridional position of East Asian westerly jet (EAWJ) is associated with rainfall anomalies in Yangtze-Huaihe River Valley (YHRV) in summer. However, the dynamic mechanism has not been resolved yet. The present study reveals underlying mechanisms for this impact for early summer and midsummer, separately. Mechanism 1: associated with EAWJ's anomalously southward displacement, the 500-hPa westerly wind over YHRV is strengthened through mid-tropospheric horizontal circulation anomalies; the westerly anomalies are related to the formation of warm advection anomalies over YHRV, which cause increased rainfall through adiabatic ascent motion and convective activities; the major difference in these processes between early summer and midsummer is the midtropospheric circulation anomaly pattern. Mechanism 2: associated with EAWJ's anomalously southward displacement, the large day-to-day variability of midtropospheric temperature advection in midlatitudes is displaced southward by the jet's trapping transient eddies; this change enhances the day-to-day variability of temperature advection over YHRV, which in turn causes the increased rainfall in most part of YHRV through "lower-bound effect" (rainfall amount can not become

negative); there is not much difference in these processes between early summer and midsummer.

Keywords East Asian westerly jet · Rainfall anomalies · Yangtze-Huaihe River Valley · Dynamic mechanisms · Asymmetric relationship · Interannual time scale

1 Introduction

The Yangtze-Huaihe River Valley (YHRV, 110°–120°E, 25°–35°N) is one of the core industrial regions throughout China. The summer rainfall is known to undergo substantial interannual variation in YHRV, which affects the socioeconomic activity (Su et al. 2013). An extensive literature exists studying the summer rainfall variation in YHRV and the causations (e.g., Zhou and Yu 2005; Zhao and Zhang 1996; Wang et al. 2013), and many achievements have been gained. Particularly, the impact of the variation in East Asian westerly jet (EAWJ) on the rainfall anomaly in YHRV attracts much attention from climate community (e.g., Lu 2004; Dong et al. 2011; Li and Zhang 2014). These studies stress the importance of the intensity and meridional position of EAWJ to the rainfall changes in YHRV. For example, the poleward (equatorial) shift of EAWJ is related to the decrease (increase) in the summer rainfall amount in YHRV (e.g., Xuan et al. 2011; Lin and Lu 2005; Liao et al. 2004; Lu 2004; Kuang and Zhang 2006). The change in EAWJ's meridional position also connects the rainfall anomaly around YHRV with the variations in other climate variables or systems such as Arctic Oscillation (AO) (Gong and Ho 2003), East Asian Monsoon (Zhao et al. 2015) and ENSO (Liang and Wang 1998).

However, dynamic mechanisms for the impact of EAWJ's meridional displacement on summer rainfall

This paper is a contribution to the special issue on East Asian Climate under Global Warming: Understanding and Projection, consisting of papers from the East Asian Climate (EAC) community and the 13th EAC International Workshop in Beijing, China on 24–25 March 2016, and coordinated by Jianping Li, Huang-Hsiung Hsu, Wei-Chyung Wang, Kyung-Ja Ha, Tim Li, and Akio Kitoh.

✉ Hongchao Zuo
zuohch@lzu.edu.cn

¹ College of Atmospheric Sciences, Lanzhou University, Lanzhou, Gansu Province, China

anomaly in YHRV remain poorly understood. Many existing studies invoked the changes in local meteorological elements such as vertical velocity and vorticity in explaining this impact (e.g., Gong and Ho 2003; Kuang and Zhang 2006). Such a discussion fails to answer a key question: how does EAWJ's meridional displacement bring about the change in these local meteorological elements? That means the dynamic mechanism has not been resolved yet. Recently, it is revealed that the EAWJ anchors the meiyu-baiu rainband by forming warm advection and steering transient eddies, which are related to the 30-day-average temperature advection and day-to-day variability of temperature advection for the 30 days in early summer (from middle June to early July) over YHRV, respectively (Sampe and Xie 2010). Based on the perspectives of these two properties of temperature advection, the mechanisms of the impact of EAWJ's meridional displacement on summer rainfall anomaly in YHRV will be explored in this research.

The rest part of the present study is organized as follows. The data and methods are briefed in Sect. 2. Section 3.1 briefs the impact of the meridional position of EAWJ on the summer rainfall in YHRV based on the data used in the present study. Sections 3.2 and 3.3 discuss the linking roles of the 30-day-average and day-to-day variability of temperature advection between EAWJ's meridional displacement and summer rainfall changes in YHRV, respectively. Section 4 provides brief conclusions and the further discussions of the results in the present study.

2 Data and methods

The present study uses the six-hourly data of zonal wind velocity, meridional wind velocity, air temperature and vertical velocity with the horizontal resolution of $2.5^\circ \times 2.5^\circ$, which were obtained from the ERA-interim reanalysis dataset (Dee et al. 2011). The daily value on each day is the average of the six-hourly data at 0000 UTC and 1200 UTC of this day. The present study also uses the rainfall observations from the 756 national basic stations throughout China, which were obtained from the China Meteorological Data Sharing Service System. These data are all for the time period 1979–2013.

Climatologically, there exists evident difference in the position of the rainband in eastern China and the pattern of circulation over East Asia between early summer and midsummer (from middle July to early August, Ding and Chan 2005; Huang et al. 2008; Zhang et al. 2006; Sampe and Xie 2010; Kosaka et al. 2011). So as usual, in the present study the summer will be separated into early summer and midsummer, i.e., the 30-day period from June 16 to July 15 and the 30-day period from July 16 to August 14, respectively.

3 Results

3.1 Impact of EAWJ's meridional displacement on summer precipitation anomalies in YHRV

The present section describes the impact of the meridional displacement of EAWJ on the summer rainfall changes in YHRV to facilitate the dynamical diagnoses in the following parts of the paper. Because the first empirical orthogonal function (EOF) pattern obtained for precipitation in YHRV shows loadings of the same sign for most of YHRV in both early summer and midsummer (figures omitted), average rainfall in YHRV is employed for correlation analysis. In early summer, significant negative correlations between the average rainfall in YHRV and 200-hPa zonal wind velocity are located north of the climatological-mean jet axis and positive correlations are located south of the jet axis (Fig. 1a). This meridional dipole of significant correlations indicates the close relationship between the meridional displacement of upper-tropospheric EAWJ and rainfall anomaly in YHRV in early summer. The results for midsummer are similar to those for early summer except for the latitude of the climatological-mean jet axis (42.5°N , Fig. 1b) and the longitude range of the dipole ($92.5^\circ\text{--}132.5^\circ\text{E}$, Fig. 1b).

To characterize EAWJ's meridional displacements, indices are defined for early summer and midsummer, respectively. Based on the latitude of the climatological-mean jet axis (37.5°N , Fig. 1a) and the longitude range of the dipole ($105^\circ\text{--}145^\circ\text{E}$, Fig. 1a), we define the difference in the average 200-hPa zonal wind velocity between $105^\circ\text{--}145^\circ\text{E}$, $27.5^\circ\text{--}37.5^\circ\text{N}$ and $105^\circ\text{--}145^\circ\text{E}$, $37.5^\circ\text{--}47.5^\circ\text{N}$ as EAWJPI for early summer. Similarly, the difference in the average 200-hPa zonal wind velocity between $92.5^\circ\text{--}132.5^\circ\text{E}$, $32.5^\circ\text{--}42.5^\circ\text{N}$ and $92.5^\circ\text{--}132.5^\circ\text{E}$, $42.5^\circ\text{--}52.5^\circ\text{N}$ is defined as EAWJPI for midsummer. Figure 1c, d show rainfall anomalies regressed onto the standardized EAWJPI in early summer and midsummer, respectively. We can observe significant positive anomalies of rainfall in most of the southern part of YHRV ($25^\circ\text{--}31^\circ\text{N}$) in early summer. In most of the northern YHRV ($31^\circ\text{--}35^\circ\text{N}$) the rainfall anomalies are also positive but not statistically significant. In midsummer, significant positive rainfall anomalies are observed between 28° and 34°N , which are much more northward than those in early summer. The rainfall anomalies are also positive in other part of YHRV except the southern margin. All the above results indicate that the southward displacement of EAWJ is related to the increased rainfall in YHRV, which is generally consistent with the results in previous studies (e.g., Fang et al. 2009; Xuan et al. 2011).

Some studies suggest that the diabatic heating generated by the rainfall can possibly change upper-tropospheric

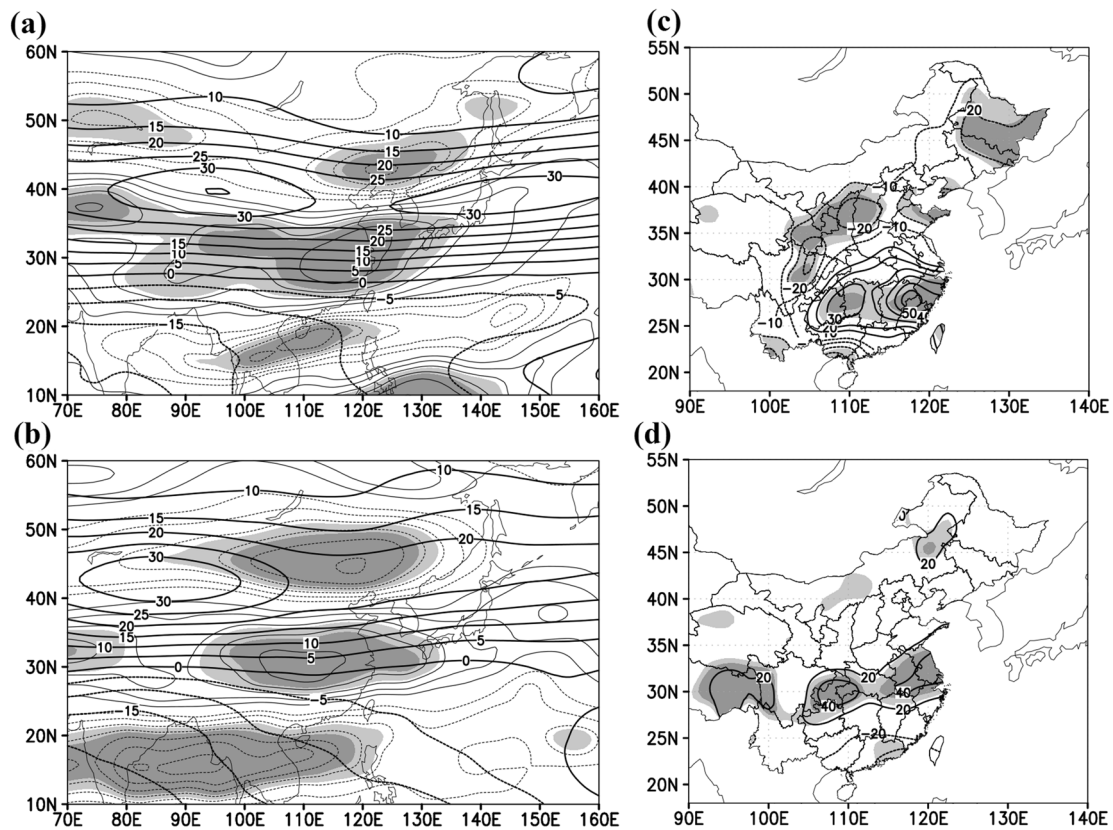


Fig. 1 **a** Climatological-mean 200-hPa zonal wind velocity (*bold lines*, in units of m/s) and correlation coefficient between 200-hPa zonal wind velocity and the average rainfall in YHRV (*light lines* at every 0.1 with *zero lines* omitted) in early summer. **c** Anomalies of rainfall (in units of mm) regressed onto standardized EAWJPI in early

summer. **b** and **d** As in **a** and **c** respectively, but for midsummer. *Light (dark) shading* represents significant level of 5% (1%), based on correlation tests. All plots were produced using Grid Analysis and Display System (GrADS) Version 2.1

circulation, which possibly affects EAWJ's meridional position (e.g. Ding and Wang 2005; Lu and Lin 2009; Chen and Huang 2012). Because the response of horizontal circulation to rainfall's condensational heating is primarily baroclinic and it minimizes in the midtroposphere, where the causality between the circulation and the diabatic heating/cooling anomalies is the easiest to interpret (Sampe and Xie 2010; Kosaka et al. 2011), the level of 500 hPa can be chosen as a standard to verify whether EAWJ's meridional displacement has an independent effect on the rainfall anomalies in YHRV. A meridional dipole of 500-hPa zonal wind velocity anomalies associated with the average rainfall in YHRV is observed around the climatological-mean 500-hPa jet axis in both early summer and midsummer (Wang and Zuo 2016, see their Fig. 1), which is similar to the result for 200 hPa (Fig. 1a, b). Based on the latitude of the jet axis and the longitude range of the dipole, the difference in average 500-hPa zonal wind velocity between 110–140°E, 22.5–32.5°N and 110–140°E, 32.5–42.5°N (110–140°E, 32.5–42.5°N and 110–140°E, 42.5–52.5°N)

is defined as the meridional position index for the 500-hPa jet, i.e. EAWJPI0, for early summer (midsummer). The removing of the EAWJPI0's influence makes the correlation between EAWJPI and average rainfall in YHRV decrease from 0.51 (0.44) to -0.09 (0.36) in early summer (midsummer). This analysis hints that at least part of the rainfall anomalies in YHRV is caused by EAWJ's meridional displacement.

3.2 Mechanism 1: connecting role of 30-day-mean temperature advection

Climatologically, the midtropospheric temperature is high in the southwest and low in the northeast over YHRV, and thus the midtropospheric southwesterly wind forms warm advection over YHRV in both early summer and midsummer (figures omitted). A simple composite technique is used to derive midtropospheric circulation changes and the associated stationary temperature advection changes with reference to EAWJ's meridional displacement. The

composite of an atmospheric variable (e.g. temperature) for high (low) EAWJPI years is the average of the variable over the years when EAWJPI is among the eight highest (lowest) values. If not specified, the phrase “stationary temperature advection” denotes the temperature advection calculated from 30-day-mean wind velocity and temperature data in this study. Regression analysis is also used in this section.

Figure 2a, b show composites of 500-hPa temperature and horizontal wind in early summer for high and low EAWJPI years, respectively. When upper-tropospheric EAWJ is displaced anomalously southward, the midtropospheric jet extending from around coastal eastern China to the northwestern Pacific area east of Japan is displaced southward correspondingly. This is related to the strengthened midtropospheric flow bypassing the southern flank of the Tibetan Plateau and merging around coastal eastern China into the midtropospheric jet. The southward displacement of the midtropospheric jet and the resultant strengthening of the midtropospheric flow originating from the southern rim of the Tibetan Plateau are related to the accelerated 500-hPa westerly wind over the YHRV together (Figs. 2a, b, 3a). Associated with the midtropospheric jet’s southward displacement, the flow bypassing the northern flank of the Tibetan Plateau is weakened and forced to turn southward over North China to merge into the jet, which results in northerly anomaly in eastern China containing the YHRV (Figs. 2a, b, 3c). When EAWJ is displaced southwards, the warm ridge over southern China also shifts slightly southwards, which is related to the anomalous negative meridional temperature gradient over YHRV (Figs. 2a, b, 3d). In the present study negative meridional temperature gradient denotes the temperature pattern that is warm in the south and cold in the north, and vice versa.

These midtropospheric circulation changes are related to stationary temperature advection anomalies over YHRV. The accelerated westerly wind over YHRV causes warm advection anomalies since the zonal temperature gradient anomaly is not statistically significant over most of YHRV (Figs. 3a, b, 4a). The negative meridional temperature gradient anomalies can not result in any significant stationary temperature advection anomalies over YHRV except the southern margin (figure omitted) because the anomalous negative meridional temperature gradient and northerly wind (Fig. 3c, d) offset each other in terms of generating stationary temperature advection anomalies.

When upper-tropospheric EAWJ is displaced anomalously southward in midsummer, the midtropospheric jet in northern China is displaced anomalously southward correspondingly (Fig. 5a, b), which is related to the accelerated midtropospheric westerly wind over YHRV (Fig. 6a). The midtropospheric warm ridge surrounding YHRV also shifts slightly more southward, which is associated with anomalous negative meridional temperature gradient over YHRV (Fig. 6d). The anomalous westerly wind over YHRV causes anomalous warm advection (Fig. 7a) since the EAWJPI-related zonal temperature gradient anomaly is not significant over most of YHRV (Fig. 6b). Also since EAWJPI-related meridional wind anomaly is not significant (Fig. 6c), the negative meridional temperature gradient anomaly can potentially cause warm advection anomaly over YHRV. However, no meridional warm advection anomaly is actually formed because the warm advection anomalies related to the negative meridional temperature gradient anomalies are mostly offset by the EAWJPI-related transient meridional cold advection anomalies over YHRV (figure omitted).

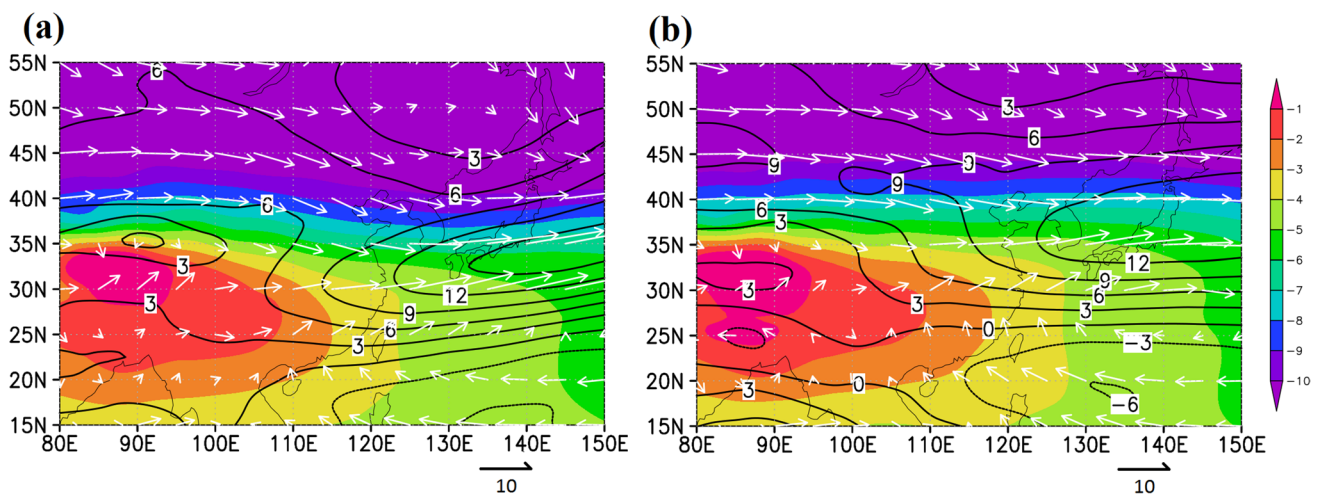


Fig. 2 Composite of 500-hPa temperature (color, in units of $^{\circ}\text{C}$), zonal wind velocity (contours, in units of m/s) and horizontal wind (arrows, in units of m/s) in early summer for **a** high EAWJPI and **b**

low EAWJPI years. Both plots were produced using Grid Analysis and Display System (GrADS) Version 2.1

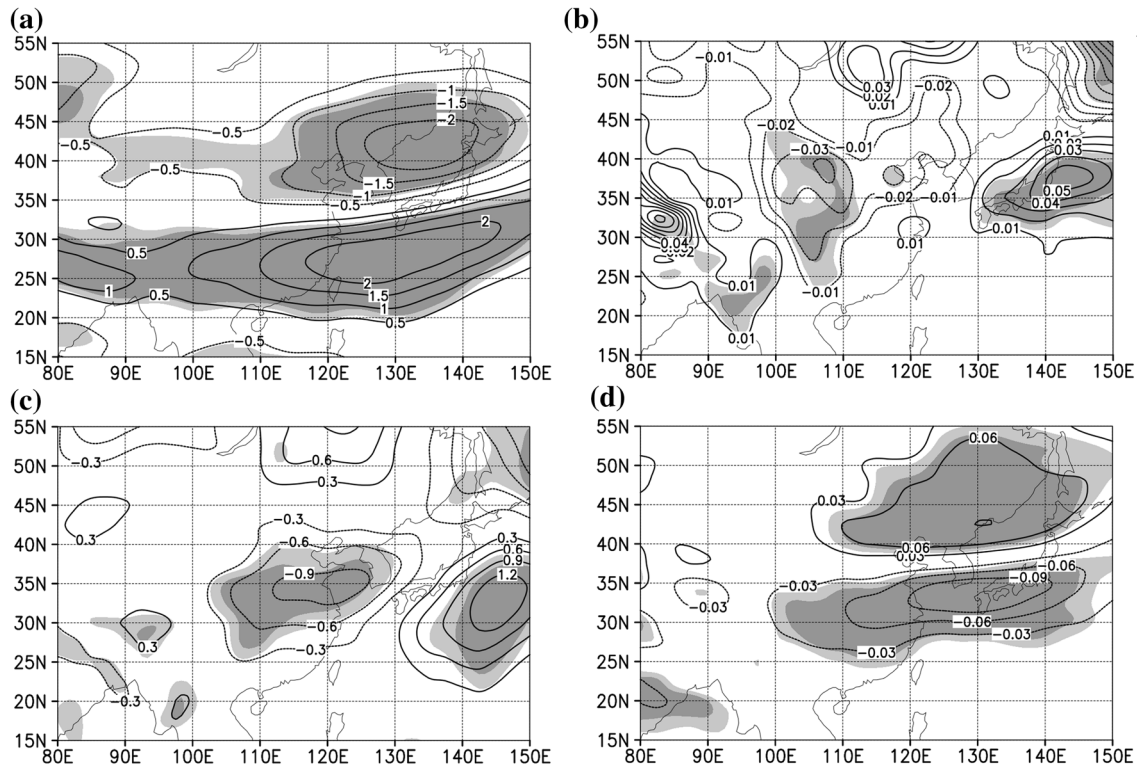


Fig. 3 Anomalies of **a** 500-hPa zonal wind velocity (m/s), **b** zonal temperature gradient (10^{-5} K/m), **c** meridional wind velocity (m/s) and **d** meridional temperature gradient (10^{-5} K/m) regressed onto the standardized EAWJPI. Dark (light) shading denotes the confidence of

0.99 (0.95), based on correlation tests. Calculation of zonal/meridional temperature gradient is as in Wang and Zuo (2016). All plots were produced using Grid Analysis and Display System (GrADS) Version 2.1

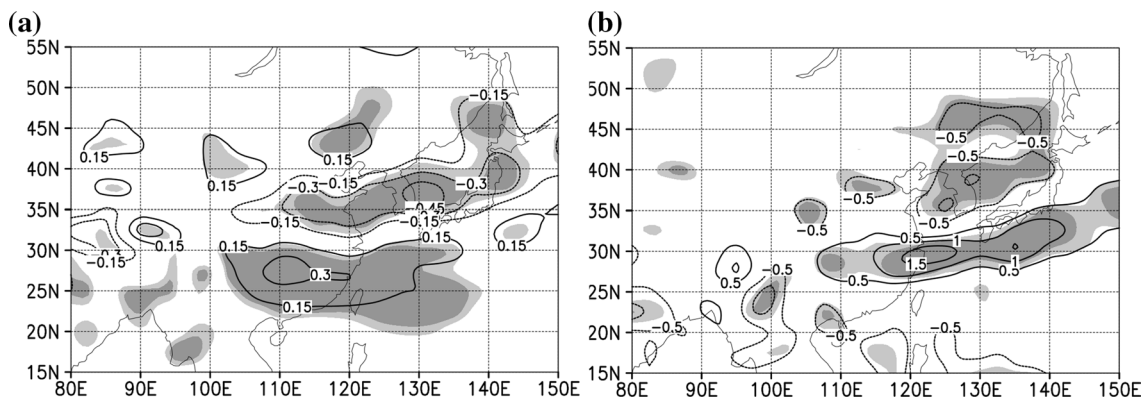


Fig. 4 As in Fig. 3 but for **a** 500-hPa stationary temperature advection (10^{-5} K/s) and **b** diabatic forcing (10^{-5} K/s)

How are the EAWJPI-related warm advection anomalies in YHRV related to the rainfall anomalies? We perform the scale-analysis of thermodynamic equation based on reanalysis data before investing into the question. The following equation is the thermodynamic equation, which is written in pressure coordinate:

$$\begin{aligned}
 -\left(-\left(\frac{p}{p_0}\right)^{R/C_p} \frac{\partial \bar{\theta}}{\partial p}\right) &= \frac{Q}{C_p} - \frac{\partial \bar{T}}{\partial t} \\
 \text{A} & \qquad \qquad \qquad \text{B} \qquad \qquad \qquad \text{C} \\
 -\bar{v} \cdot \nabla_p \bar{T} - \overline{v' \cdot \nabla_p T'} - \left(\frac{p}{p_0}\right)^{R/C_p} \overline{\omega' \frac{\partial \theta'}{\partial p}} & \qquad \qquad \qquad \text{D} \qquad \qquad \qquad \text{E} \qquad \qquad \qquad \text{F}
 \end{aligned} \tag{1}$$

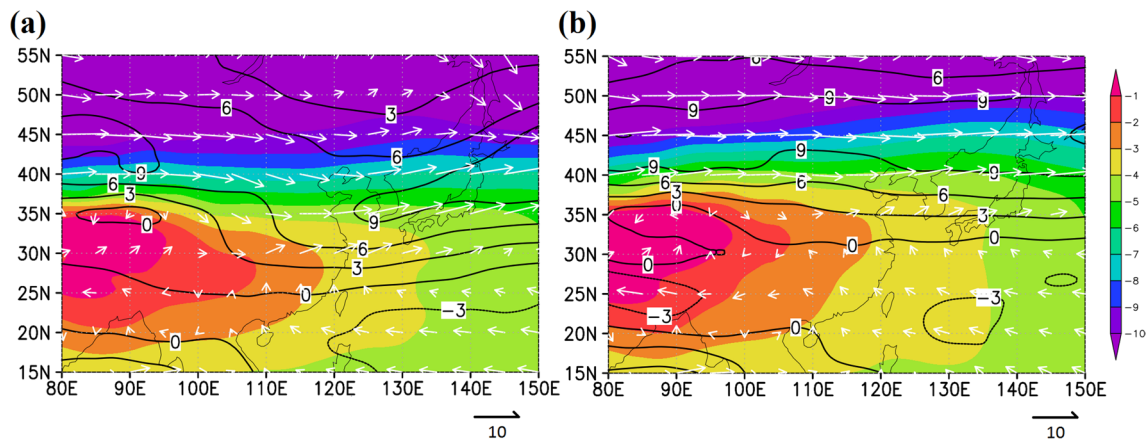


Fig. 5 As in Fig. 2 but for midsummer

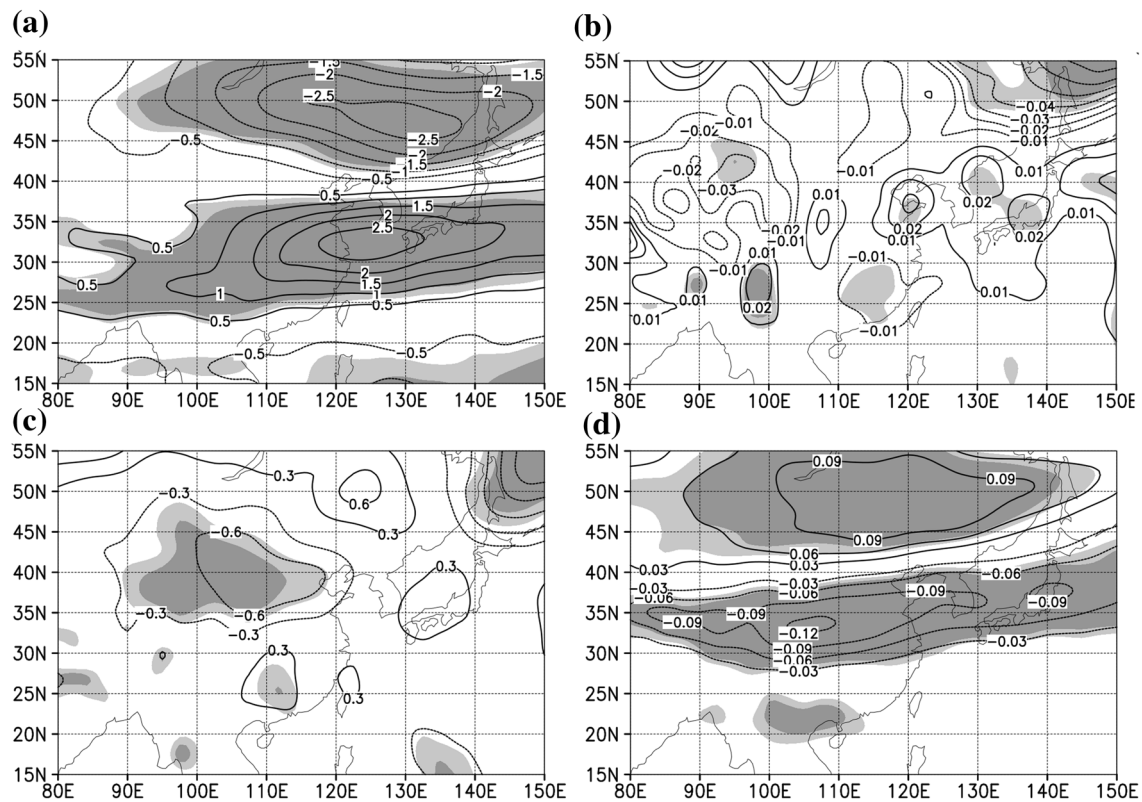


Fig. 6 As in Fig. 3 but for midsummer

where the capital letters under the equation denote terms (the sign included). Other notations are the same as those in Sampe and Xie (2010).

The temperature tendency term (C) can be neglected (Sampe and Xie 2010) in seasonal scale. In both early summer and midsummer, the magnitude of standard deviation of $\frac{\partial \bar{\theta}}{\partial p}$ is an order smaller than the magnitude of the

climatology of $\frac{\partial \bar{\theta}}{\partial p}$, while the magnitude of standard deviation of vertical velocity has the same order as the magnitude of the climatological-mean vertical velocity over YHRV (figures omitted). This contrast suggests that the variance of vertical advection term (A) is mainly determined by the variance of vertical velocity, namely, variables associated with the vertical advection anomaly over

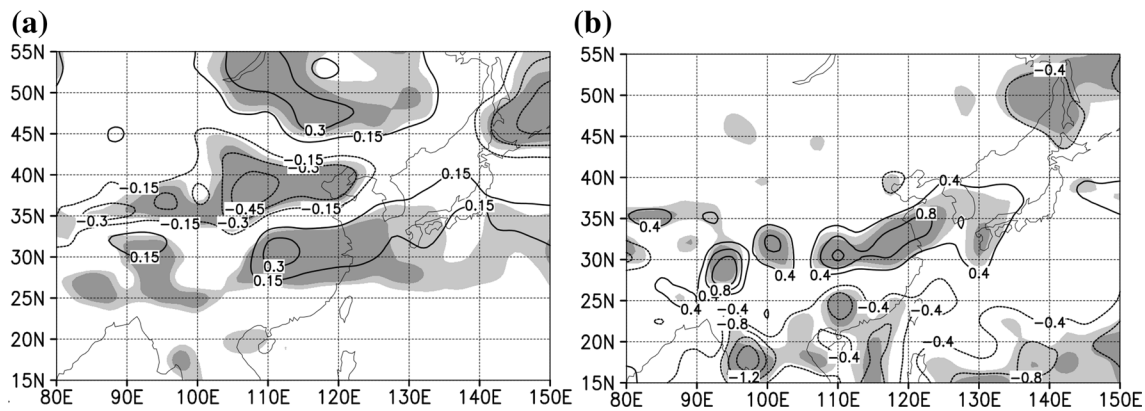


Fig. 7 As in Fig. 4 but for midsummer

YHRV are also related to the vertical velocity anomaly, which can be used to describe rainfall anomaly (Lu and Lin 2009).

The remaining terms on the two sides of the equation are diabatic heating/cooling term (B), stationary temperature advection term (D), transient temperature advection term (E) and transient vertical advection term (F). To estimate their roles in changing rainfall, we calculate these terms' interannual standard deviations at 500 hPa, (figure omitted). The variance of term B is one order of magnitude larger than the variance of terms D, E and F over YHRV in both early summer and midsummer, indicating that the predominant balance is between the variance of vertical advection and that of diabatic heating/cooling over YHRV. Therefore, diabatic heating/cooling term is one of our focuses in the rest of this section. Rainfall anomalies directly cause diabatic heating/cooling anomalies. In order to resolve the mechanisms between horizontal circulation and rainfall anomalies, we should also focus on the terms directly related to horizontal circulation changes but not directly impacted by rainfall anomalies. The stationary and transient temperature advection terms (D+E) satisfy the two conditions, while transient vertical advection changes are susceptible to local rainfall anomalies. Thus, we also focus on D and E.

The EAWJPI-related warm advection anomalies can cause adiabatic ascent and associated positive rainfall anomalies. Wang and Zuo (2016) revealed that daily diabatic heating/cooling changes associated with the daily temperature advection changes over YHRV are stronger (weaker) and located more eastward (westward) when the temperature advection leads (lags) the diabatic heating/cooling by 1 day than when the daily temperature advection is concurrent with diabatic heating/cooling. Based on this result, they concluded that the warm (cold) advection anomalies over YHRV cause diabatic heating (cooling) anomalies through triggering convection. The anomalous

diabatic heating is primarily associated with anomalous rainfall. Thus, the EAWJPI-related warm advection anomalies can also cause positive rainfall anomalies in YHRV through triggering convective feedback (Figs. 4b, 7b).

A careful comparison between EAWJPI-related stationary temperature advection and diabatic heating/cooling tends to be centered slightly northeast of the anomalous stationary temperature advection over YHRV in both early summer and midsummer (Figs. 4, 7). These discrepancies suggest that there would be some other factors affecting the diabatic heating anomalies over YHRV besides the warm advection anomalies.

The role of transient temperature advection in connecting the rainfall anomalies in YHRV and EAWJ's meridional displacement is analyzed by regressing 500-hPa transient temperature advection onto standardized EAWJPI for early summer and midsummer (figures omitted). The EAWJPI-related transient temperature advection anomalies over YHRV are overall opposite in sign to the stationary temperature advection anomalies (Figs. 4a, 7a). But the former's magnitude is only about one-third of the latter's magnitude. This suggests that the transient temperature advection anomalies offset a small part of the stationary temperature advection anomalies and thus slightly weaken the latter's connecting role.

3.3 Mechanism2: connecting role of day-to-day variability of midtropospheric temperature advection

Composites of 200-hPa zonal wind velocity and day-to-day standard deviation of 500-hPa temperature advection for high and low EAWJPI years are calculated to derive the upper-tropospheric circulation changes and the associated changes in day-to-day variability of midtropospheric temperature advection with reference to the meridional

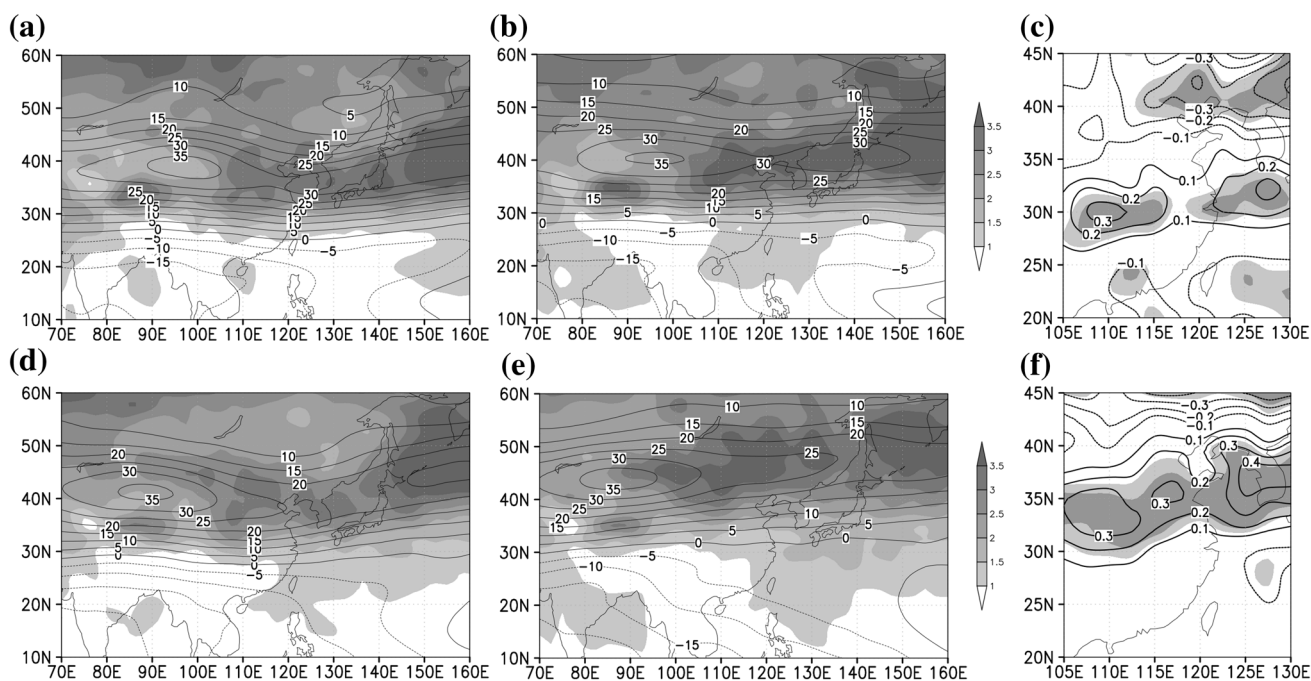


Fig. 8 Composite of 200-hPa zonal wind velocity (contours, in units of m/s) and day-to-day standard deviation of 500-hPa temperature advection (color, 10^{-5} K/s) for **a** high EAWJPI and **b** low EAWJPI early summers. **c** Regression coefficients of day-to-day standard deviation of 500-hPa temperature advection (contours, in units of 10^{-5} K/s) upon standardized EAWJPI for early summer. **d–f** As in (a)–(c)

but for midsummer. *Dark (light) shading* in (c) and (f) denotes the confidence of 0.99 (0.95), based on correlation tests. The day-to-day standard deviations of 500-hPa temperature advection are calculated from the daily data. All plots were produced using Grid Analysis and Display System (GrADS) Version 2.1

displacement of EAWJ (Fig. 8a, b, d, e). The day-to-day standard deviation of 500-hPa temperature advection for each early summer/midsummer is calculated from the daily temperature advection data for the 30 days in this early summer/midsummer. The day-to-day variability actually includes two components: synoptic variability (2–8 days) and intraseasonal oscillations (10–30 days). The comparison shows that the synoptic variability accounted for about 90 percent of the total day-to-day variability in most of YHRV. So, most of the rainfall changes related to day-to-day variability of 500-hPa temperature advection, which will be revealed in the present section, are the results of the synoptic variability of 500-hPa temperature advection.

As shown in the figure, in both early summer and midsummer and for both high and low EAWJPI years the high day-to-day variability of temperature advection at 500 hPa is almost collocated with the westerly jet at 200 hPa in the region extending from the middle and eastern part of China toward the Pacific area east of Japan. In western China (west of 105°E) the collocation is somewhat ambiguous. The poor correspondence may be due to the existence of the Tibetan Plateau, whose top can reach the middle troposphere. Those results suggest the essential role of the upper-tropospheric jet system in the formation of the large day-to-day variability of midtropospheric temperature

advection. As indicated by Sampe and Xie (2010), the large day-to-day variability of midtropospheric temperature advection is related to the transient eddies trapped by 200-hPa westerly jet. Thus, the anomalously southward displacement of EAWJ can result in the anomalously southward displacement of the region with high day-to-day variability of midtropospheric temperature advection in middle-eastern East Asia by trapping transient eddies. This change in turn increases the day-to-day variability of midtropospheric temperature advection over YHRV in early summer and midsummer. Figure 8c, f exhibit the changes in the day-to-day standard deviation of 500-hPa temperature advection with reference to the meridional displacement of EAWJ in early summer and midsummer, respectively. As shown in the figures, significant increase in the day-to-day variability of midtropospheric temperature advection is observed along the latitude of 30°N in early summer, while in midsummer the significant increase is observed over the northern YHRV and no significant change is observed over the southern YHRV. These results are consistent with the ones obtained from the composite analyses.

The day-to-day variability of midtropospheric temperature advection can impact the rainfall in early summer and midsummer through the lower bound effect of rainfall. Daily midtropospheric temperature advection is

significantly positively correlated with rainfall both for the days in early summer and for the days in midsummer (figure omitted). In the days with strong warm advection over YHRV, the adiabatically induced ascent generates heavy rainfall through the moisture feedback, while in the days when cold (strong cold) advection prevails over YHRV, the adiabatically induced descent should cause negative (large negative) value of rainfall. Because rainfall cannot be negative, the lower bound effect increases the value of rainfall from the imaginary negative (large negative) value to a real zero value in the days with cold advection. Under these circumstances, even though due to other weather variability daily rainfall is suppressed in some warm-advection days and rainfall happens in some cold-advection days,

the frequency of zero-rainfall days should be much larger for cold-advection days than for warm-advection days in YHRV, which is consistent with the observations (Fig. 9). At the same positive 30-day-average temperature advection over YHRV, there tend to be more days with cold advection or strong cold advection for the early summer/midsummer with anomalous stronger day-to-day variability of midtropospheric temperature advection, which is consistent with the observations over YHRV (Fig. 10). Thus, for this kind early summer/midsummer the rainfall increase associated with the lower-bound effect tends to be anomalously more, which leads to the more 30-day-total rainfall.

In order to confirm the above-mentioned mechanism, the relationship of the rainfall in YHRV with the day-to-day

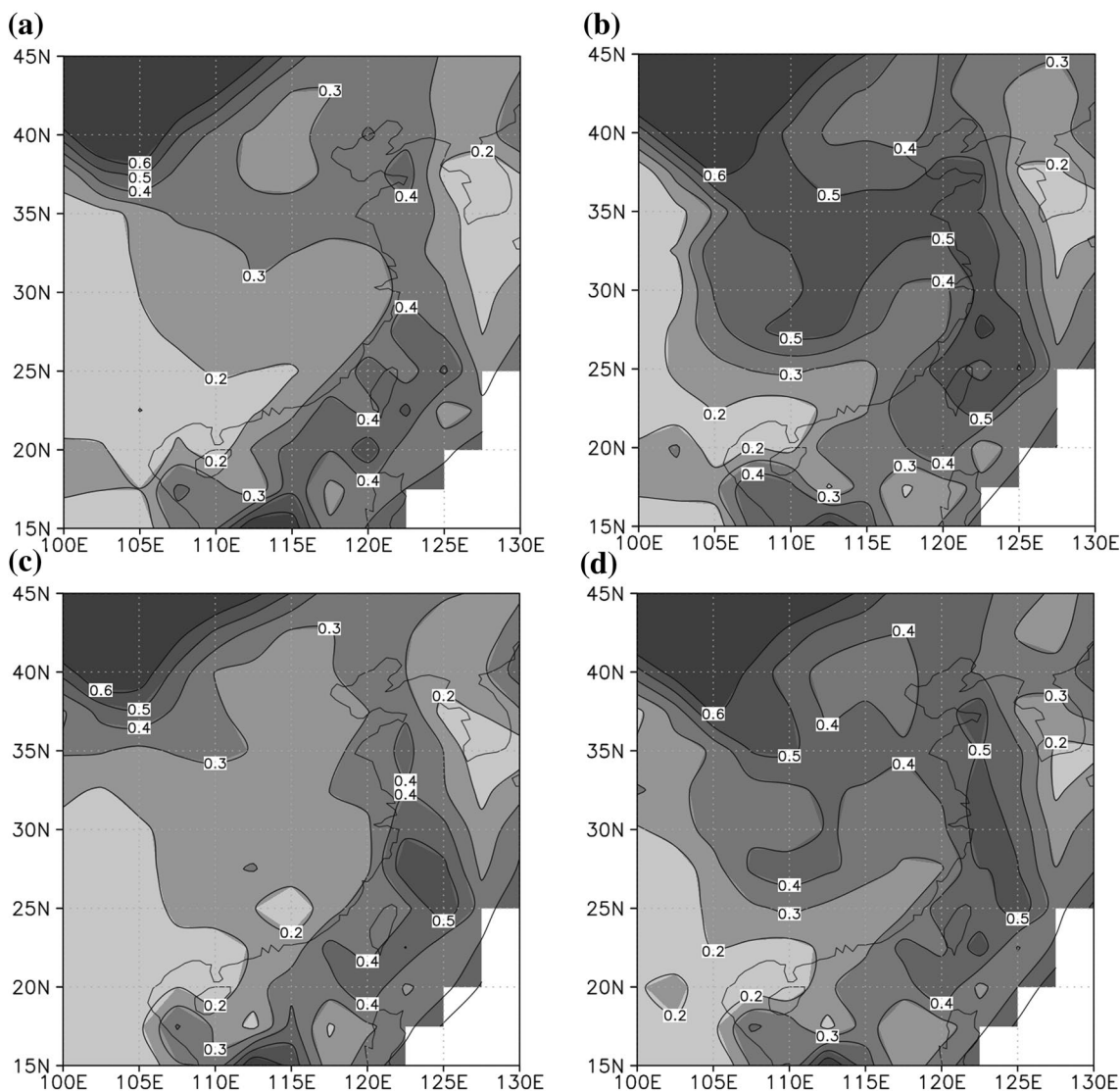


Fig. 9 Fraction of zero-rainfall days for early summer days with **a** warm advection and **b** cold advection at 500 hPa. The daily gridded rainfall data is obtained by interpolating station rainfall data into regular grids of 2.5° lat×2.5° lon using Cressman interpolation. The

fractions are acquired by categorizing the 1050 early summer days into two kinds based on signs of temperature advection at each grid point and then calculating the fraction of the zero-rainfall days for each kind at this point. **c–d** As in (a)–(b) but for midsummer days

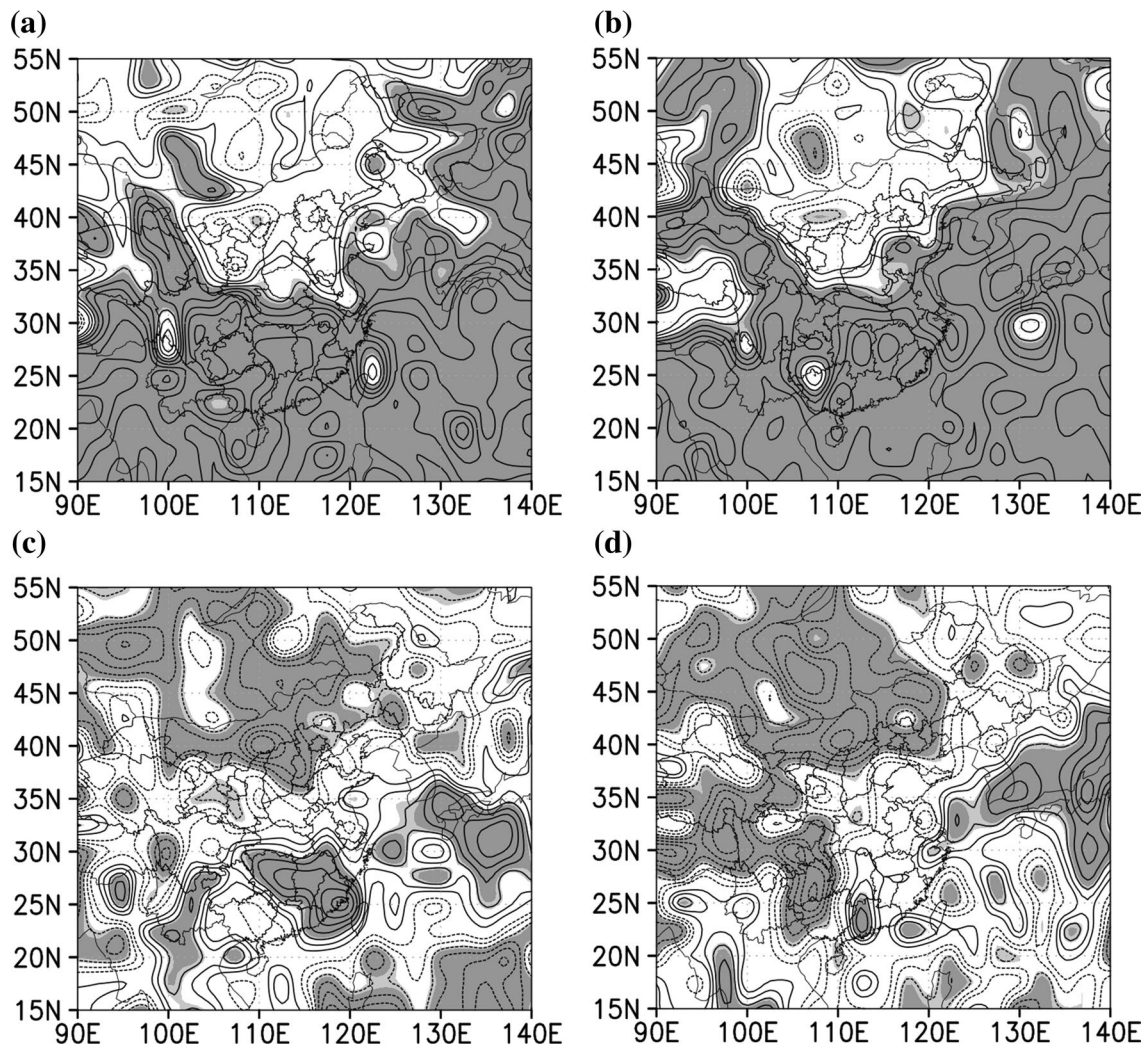


Fig. 10 **a** Partial correlation between the number of the days with strong cold advection (less than -1.0×10^{-5} K/s) and day-to-day standard deviation of 500-hPa temperature advection at the same grid point for early summers. The influence of the 30-day-average temperature advection has been removed in calculating the partial correla-

tion. **b** As in (a) but for midsummers. **c–d** As in (a)–(b) but for the number of the days with cold advection (less than -0.0×10^{-5} K/s). *Dark (light) shading* denotes the confidence of 0.99 (0.95). The contour interval is 0.1 and the contour line of zero is omitted. *Dashed lines* denote the negative correlation

variability of temperature advection is analyzed using the observations. Based on the region with significant EAWJPI-related anomalies of day-to-day variability of midtropospheric temperature advection in early summer and midsummer (Fig. 8c, f), the rainfall, the 30-day-average and the day-to-day variability of 500-hPa temperature advection are averaged over 110–120°E, 27.5–32.5°N for early summer and over 110–120°E, 30–35°N for midsummer. Regressions of the region-mean rainfall upon the region-mean day-to-day variability of temperature advection are calculated. When calculating the regressions the variances associated with the region-mean 30-day-average temperature advection are removed from the two series in recognition that rainfall is closely correlated with the 30-day-average temperature advection. The increases in

region-mean rainfall associated with one standard deviation increase in the region-mean day-to-day variability of temperature advection are 54 and 43 mm for early summer and midsummer, respectively, which are both significant at 0.95 confidence level based on correlation tests (Fig. 11). They are comparable in magnitude to the region-mean rainfall changes associated with one standard deviation increase in the region-mean of 30-day-average temperature advection, which are 83 and 55 mm, respectively. These results suggest that the positive influence of the day-to-day variability of midtropospheric temperature advection on the rainfall in YHRV revealed theoretically in the last paragraph is consistent with observations and non-negligible in changing rainfall in YHRV.

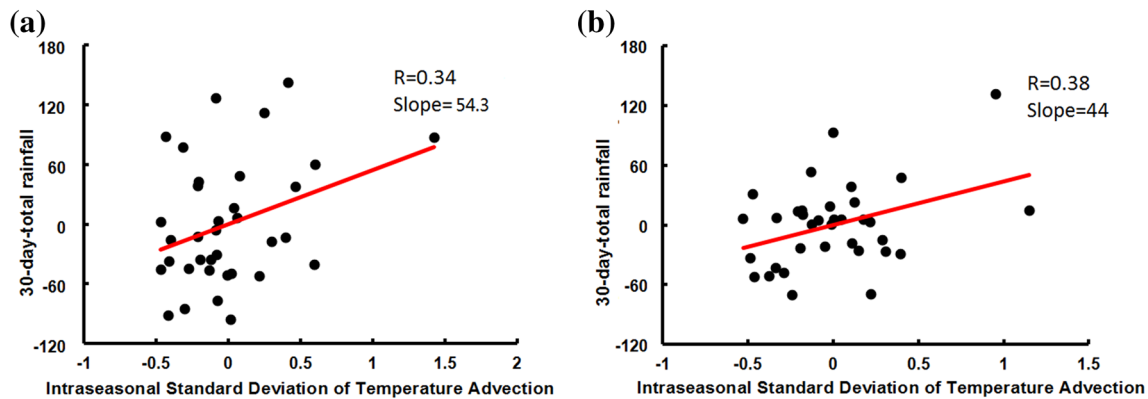


Fig. 11 **a** Scatter plot of 30-day-total rainfalls averaged over 110–120°E, 27.5–32.5°N against the day-to-day standard deviation of 500-hPa temperature advection averaged over the same region for early summer. The variance associated with the 30-day-average temperature advection averaged over the same region has been removed from

the two series (region-mean rainfall and day-to-day standard deviation of 500-hPa temperature advection). A set of linear regression statistics (correlation and slope) is shown on the upper-right corner of the panel. **b** As in (a) but for midsummer and 110–120°E, 30–35°N. Both plots were produced using Microsoft Excel 2007

The EAWJPI-related anomalies of the day-to-day variability of 500-hPa temperature advection (Fig. 8c, f) are with the same order of magnitude as the anomalies of 500-hPa stationary temperature advection over YHRV (Figs. 7a, 4a). Thus, the EAWJPI-related anomaly of day-to-day variability of temperature advection over YHRV can result in substantial local rainfall changes (Fig. 8c, f) through the lower-bound effect. In early summer rainfall increase is observed in the northern YHRV (110–120°E, 31–35°N) where cold advection anomaly prevails (Fig. 1c). The contrast between anomalous rainfall and temperature advection may be associated with the EAWJ-related increase in the day-to-day variability of temperature advection (Fig. 8c) in this region. In midsummer, EAWJPI-related increase in the day-to-day variability of temperature advection (Fig. 8f) is located in the northern YHRV. It makes the significant positive rainfall anomalies (Fig. 1d) be located slightly more northward than the significant positive warm advection anomalies (Fig. 7a), which are observed in the central part of YHRV.

4 Conclusions and summaries

The meridional displacement of EAWJ significantly impacts summer rainfall anomalies in YHRV and our results reveal two dynamic mechanisms responsible for this impact. In early summer, the southward displacement of 200-hPa EAWJ is associated with the southward displacement of the midtropospheric jet extending from around coastal eastern China eastwards to east of Japan, which strengthens the midtropospheric flow originating from the southern boundary of Tibetan Plateau. The southward displacement of the midtropospheric jet and the resultant strengthening of the midtropospheric flow

together speed up the westerly wind over YHRV. In midsummer, the westerly jet is displaced southward from upper-troposphere to midtroposphere, which also speeds up the midtropospheric westerly wind over YHRV. Since the climatological-mean midtropospheric temperature is high in the southwest and low in the northeast, the increased midtropospheric westerly wind causes anomalous warm advection over YHRV in both early summer and midsummer. The warm advection anomalies cause anomalous rainfall rise in YHRV through inducing adiabatic ascent and triggering convection activities.

The southward displacement of 200-hPa EAWJ is also associated with the southward displacement of the large day-to-day variability of 500-hPa temperature advection because the upper-tropospheric jet stream can trap midtropospheric transient eddies. These changes can result in the increased day-to-day variability of 500-hPa temperature advection over most of YHRV. The enhanced day-to-day variability of 500-hPa temperature advection has positive effect on the rainfall in YHRV because the larger day-to-day variability of 500-hPa temperature advection is related to more days with cold advection or extremely cold advection but the daily rainfall amount can not become negative. With this effect, the EAWJPI-related increase in the day-to-day variability of midtropospheric temperature advection contributes to the rainfall increase in YHRV for both early summer and midsummer.

The present study reveals two mechanisms for the impact of the EAWJ's meridional displacement on the rainfall anomaly in YHRV, which can provide the physical basis for and thus confirm the robustness of the well-known impact of the EAWJ's variation on the rainfall anomalies. The two mechanisms can also help more comprehensively understand the formation and change of droughts and

floods occurring in YHRV. In the analysis of the second of the two mechanisms, the present study shows that the changes in the day-to-day variability of midtropospheric temperature advection can impact the 30-day-total rainfall in summer because the daily rainfall can not become negative. This provides a new perspective on the study of the dynamic processes associated with rainfall anomalies.

It is noticed that the summer rainfall regime in the eastern part of China demonstrates several interdecadal shifts during the past decades (e.g., Ding et al. 2008; Gong and Ho 2002; Huang et al. 2013) and the interdecadal changes in EAWJ's meridional position are related to these shifts (Xuan et al. 2011). It needs further study to test whether the mechanisms revealed in the present study still work for the interdecadal relationship between EAWJ's meridional displacement and the rainfall anomaly in YHRV.

The feedback mechanism widely exists in the earth system, and jet also likely interacts with precipitation. The meridional displacement of 200-hPa EAWJ affects the midtropospheric 30-day-mean temperature advection anomalies mainly through the meridional position changes of the midtropospheric jet. We have also calculated the anomalies of the day-to-day variability of midtropospheric temperature advection associated with EAWJPIO, and found out that the results are similar to those shown in Fig. 8d, f for both early summer and midsummer. These two facts suggest that the two mechanisms revealed in the present study are at least partly independent of the response of the upper-tropospheric circulation changes to diabatic heating associated with the rainfall in YHRV.

Acknowledgements The authors wish to thank the two anonymous reviewers for comments that help greatly improve the manuscript, especially on the description of the processes linking the day-to-day variability of midtropospheric temperature advection and the rainfall changes. This work was supported by National Basic Research Program of China (Grant No. 2012CB956202), National Natural Science Foundation of China (Grant No. 41275019, 41475009) and the Fundamental Research Funds for the Central Universities (Grant No. lzujbky-2016-195). The reanalysis data are obtained from <http://apps.ecmwf.int/datasets/data/interim-full-daily/levtype=sfc/> and the rainfall observations are obtained from <http://ncc.cma.gov.cn/>.

Open Access This article is distributed under the terms of the Creative Commons Attribution 4.0 International License (<http://creativecommons.org/licenses/by/4.0/>), which permits unrestricted use, distribution, and reproduction in any medium, provided you give appropriate credit to the original author(s) and the source, provide a link to the Creative Commons license, and indicate if changes were made.

References

- Chen G, Huang R (2012) Excitation mechanisms of the teleconnection patterns affecting the July precipitation in Northwest China[J]. *J Clim* 25(22):7834–7851
- Dee DP, Uppala SM, Simmons AJ et al (2011) The ERA-interim reanalysis: configuration and performance of the data assimilation system. *Q J Roy Meteor Soc* 137:553–597
- Ding Y, Chan CLJ (2005) The East Asian summer monsoon: an overview. *Meteorol Atmos Phys* 89:117–142
- Ding Q, Wang B (2005) Circumglobal teleconnection in the northern hemisphere summer. *J Climate* 18(17):3483–3505
- Ding Y, Wang Z, Sun Y (2008) Inter-decadal variation of the summer precipitation in East China and its association with decreasing Asian summer monsoon Part I: observed evidences. *Int J Climatol* 28:1139–1161
- Dong L, Guo P, Wang P, Li Q (2011) Impact of the variation of westerly wind jets over East Asia on precipitation of eastern China in July. *Sci Cold Arid Reg* 3:408–418
- Fang X, Zeng X, Chen X (2009) Spatial and temporal distribution characteristics of westerly wind Jet in 200-hPa in East Asia and the analysis of relationship between it and summer precipitation in China. *Meteorol Environ Sci* 32:11–15
- Gong DY, Ho CH (2002) Shift in the summer rainfall over the Yangtze River valley in the late 1970s. *Geophys Res Lett* 29:78-1-78-4
- Gong D, Ho CH (2003) Arctic oscillation signals in the East Asian summer monsoon. *J Geophys Res-Atmos* 108:14-1-14-6
- Huang R, Gu L, Chen J, Huang G (2008) Recent progresses in studies of the temporal-spatial variations of the East Asian monsoon system and their impacts on climate anomalies in China (in Chinese). *Chin J Atmos Sci* 32:691–719
- Huang RH, Liu Y, Feng T (2013) Interdecadal change of summer precipitation over Eastern China around the late-1990s and associated circulation anomalies, internal dynamical causes. *Chin Sci Bull* 58:1339–1349
- Kosaka Y, Xie SP, Nakamura H (2011) Dynamics of interannual variability in summer precipitation over East Asia. *J Clim* 24:5435–5453
- Kuang X, Zhang Y (2006) Impact of the position abnormalities of East Asian subtropical westerly wind jet on summer precipitation in middle-lower reaches of Yangtze River. *Plateau Meteorol (in Chinese)* 25:382–389
- Li L, Zhang Y (2014) Effects of different configurations of the East Asian subtropical and polar front jets on precipitation during the mei-yu season. *J Clim* 27:6660–6672
- Liang X, Wang W (1998) Associations between China monsoon rainfall and tropospheric jets. *Q J Roy Meteor Soc* 124: 2597–2623
- Liao QH, Gao ST, Wang HJ, Tao S (2004) Anomalies of the extratropical westerly Jet in the north hemisphere and their impacts on east Asian summer monsoon climate anomalies. *Chin J Geophys (in Chinese)* 47:10–18
- Lin Z, Lu R (2005) Interannual meridional displacement of the East Asian upper-tropospheric jet stream in summer. *Adv Atmos Sci* 22:199–211
- Lu R (2004) Associations among the components of the East Asian summer monsoon system in the meridional direction. *J Meteorol Soc Jpn* 82:155–165
- Lu R, Lin Z (2009) Role of subtropical precipitation anomalies in maintaining the summertime meridional teleconnection over the western North Pacific and East Asia. *J Clim* 22(8):2058–2072
- Sampe T, Xie SP (2010) Large-scale dynamics of the meiyu-baiu rainband: Environmental forcing by the westerly wind jet. *J Clim* 23:113–134
- Su T, Zhang S, Zhi R, Chen J (2013) Summer precipitation response to the length of the preceding winter over yangtze-huaihe river valley. *Acta Phys Sin* 62:69203-1-069203-9
- Wang S, Zuo H (2016) Effect of the East Asian Westerly Jet's intensity on Summer rainfall in the Yangtze River valley and its mechanism. *J Clim* 29:2395–2406
- Wang D, Zhang Y, Huang A (2013) Climatic features of the south-westerly wind low-level jet over southeast china and its

- association with precipitation over east China. *Asia-Pac. J Atmos Sci* 49:259–270
- Xuan S, Zhang Q, Sun S (2011) Anomalous midsummer rainfall in Yangtze River-Huaihe River valleys and its association with the EAJ. *Adv Atmos Sci* 28:387–397
- Zhang Y, Kuang X, Guo W, Zhou T (2006) Seasonal evolution of the upper - tropospheric westerly jet core over East Asia. *Geophys Res Lett* 33:L11708
- Zhao H, Zhang X (1996) The relationship between the Summer Rain-Belt in China and the East Asia Monsoon. *Meteorol Monthly (in Chinese)* 22:8–12
- Zhao G, Huang G, Wu R, Wu R, Tao W, Gong H, Qu X, Hu K (2015) A new upper-level circulation index for the East Asian Summer monsoon variability. *J Clim* 28:9977–9996
- Zhou TJ, Yu RC (2005) Atmospheric water vapor transport associated with typical anomalous summer rainfall patterns in China. *J Geophys Res-Atmos* 110:D8